Structural Engineering and Mechanics, Vol. 10, No. 6 (2000) 561-575
DOI: http://dx.doi.org/10.12989/sem.2000.10.6.561

Protective systems for high-technology facilities against microvibration and earthquake

Jann N. Yang†

Department of Civil & Environmental Engineering, University of California, Irvine, CA 92697, U.S.A.

Anil K. Agrawal‡

Department of Civil Engineering, The City College of the City University of New York, NY, U.S.A.

Abstract. Microvibration of high technology facilities, such as semiconductor plants and facilities with high precision equipments, due to nearby road and rail traffic has attracted considerable attention recently. In this paper, a preliminary study is conducted for the possible use of various protective systems and their performance for the reduction of microvibration. Simulation results indicate that passive base isolation systems, hybrid base isolation systems, passive floor isolation systems, and hybrid floor isolation systems are quite effective and practical. In particular, the performances of hybrid floor isolation systems are remarkable. Further, passive energy dissipation systems are not effective for the reduction of microvibration. Finally, the protections against both microvibration and earthquake are also investigated and presented.

Key words: microvibration; protective systems; high technology facilities; vibration control; seismic response control.

1. Introduction

Many high technology facilities, such as integrated circuits manufacturing factories, laser and optical equipments, etc., are susceptible to microvibration due to man-made environmental loads. These include the excitations from mechanical equipment in the buildings (e.g. fans, pumps, compressors, etc.) and excitations transmitted from external sources, such as nearby road and rail traffic, machinery, and constructions. Recently, microvibration of high technology facilities resulting from nearby traffic loads has attracted considerable attention (e.g., Ho 1997, Liu 1998, Andow and Ogawa 1998, Heiland and Beyer 1998, Iseki 1997, Ungar *et al.* 1990, etc.). Plant design criteria have been proposed for different types of facilities in terms of the velocity spectrum of the floor as shown in Fig. 1 (e.g., Gordon 1991). The floor velocity spectrum can be computed based on the structural dynamic analysis for given structural properties and site excitations (at the building base). The site excitation, on the other hand, can be obtained either by measurements or by computation based on the finite-element wave propagation analysis for given excitation sources (e.g., moving train) (e.g. Krylov 1996, Yang 1998).

† Professor
‡ Assistant Professor

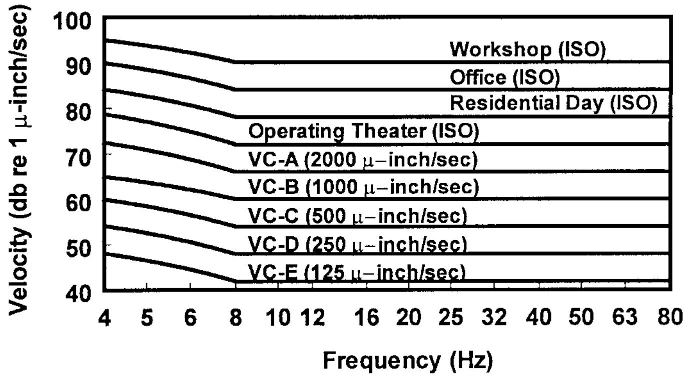

Fig. 1 Generic vibration criteria (VC) curves for vibration sensitive equipment

For the reduction of the floor response to satisfy the design specification, one possible solution is to reduce the intensity of the site excitation either by locating the facilities far away from the roads and railway tracks or by using other strategies such as wave barriers (e.g., Takemiya and Kellezi 1998, Yang 1998, Nelson 1996). Another possible solution is to reduce the floor response by installing the protective systems for the building or floor (e.g., Yang and Agrawal 1998, 1999). In this paper, we conduct a preliminary study on the reduction of the floor response due to microvibration using various protective systems, including passive and hybrid protective systems. Likewise, the reduction of floor and building responses against both microvibration and earthquake are also investigated. Microvibration of floors and buildings consists of horizontal and vertical components. In this preliminary study, we investigate only the reduction of the horizontal component, whereas the protection against the vertical component of microvibration can be made in a similar manner.

2. Train-induced ground motions

Ground motions induced by high-speed trains can propagate through the surrounding soils to adjacent buildings. The mechanism of vibration generation as well as propagation depends on the soil profile, structural supports for the tracks, (e.g., tracks directly mounted on ground, tracks on viaducts, etc.), speed of train, number of cars in a train, wheel distance in cars, etc. An early work on ground motions due to passing trains was presented by Dawn and Stanworth (1979), in which the mechanism of train-induced ground motion was described based on the concept of changing stress field. The stress field due to the static weight of moving trains is modified by unsprung masses, the suspension characteristics of railway cars, speed, type of foundation support for the tracks, etc. The changing stress field is propagated from the tracks through the ground motion by (i) compression waves, with particle motion in the direction of propagation, (ii) shear waves, with particle motion in a plane normal to the direction of propagation, and (iii) Rayleigh waves, with particle motion in an elliptical plane through the direction of propagation. However, because of different geometric attenuation of these waves, the Rayleigh waves carry most of the energy at significant distances away from the track. Moreover, high frequencies are attenuated more rapidly than low frequencies, so that low frequencies dominate the spectrum at far distances from the source. The dominant frequency of ground vibration generally lies in the range of 4 to 30 Hz. Verhas (1979) proposed various models for predicting the propagation of train-induced ground motion, including compression waves, shear waves and Rayleigh waves, and models for geometrical attenuation. His results indicated that the energy propagated in the soil is dominated by low frequencies, with the peak occurring mainly in the region of 10-20 Hz.

Recently, the prediction of train-induced ground motion has been studied analytically by many investigators. Kuppelwieser and Ziegler (1996) discussed the development of a computer database, VIBRA 1-2-3, which can be used to extrapolate ground vibration data for a particular site from a measured database. Hunt (1996) presented a stochastic approach to calculate vibration spectra at building site by modelling railway track forces as a line of vertical forces acting through the ground along an infinite straight line. Jones and Block (1996) presented an analytical model for the prediction of ground vibration from freight trains. In this model, the vibration prediction was made by considering combined effects of dynamic forces due to unevenness of the track and the effect of track deformation under successive axle loads. Their investigation shows that heavy freight trains cause ground vibration with predominant frequencies in the range of 4-30 Hz. Madshus *et al.* (1996) proposed a semi-empirical model for predicting low frequency vibration on soft ground, based on a large number of vibration measurements in Sweden and Norway. Heckl *et al.* (1996) presented an extensive description of the mechanism for the generation and propagation of ground motions. His results show that the train-induced ground vibrations have peak velocity levels in the range of 0-80 Hz. For railway tracks on ballast foundations, the predominant vibration is caused by the resonance of the wheel mass against the stiffness of the track.

In soft soil regions, railway tracks are generally supported on viaducts, which in turn are supported on piles. Takemiya (1998) investigated the characteristics of measured ground vibrations for railway tracks on flat ground, mounted tracks on embankments, and mounted tracks on viaducts. For railway tracks on flat ground, the Fourier spectrum of ground acceleration measured near the tracks contains frequency components in the range of 0 to 50 Hz. However, both low and high frequency components are damped out as the distance from the track increases. Ground acceleration measurements at a distance of 25 m from the track contains frequency components in the range of 10 to 30 Hz. For the railway track on the viaduct, the dominant frequency components at 25 m from the track are in the range of 10 to 30 Hz.

The prediction of train-induced ground motion requires extensive modeling for railway cars, tracks, track bed, and surrounding soil media. In this paper, the horizontal ground acceleration is modelled by an uniformly modulated nonstationary random process for simplicity. A sample of stationary acceleration time-history for the horizontal ground acceleration will be simulated using the modified Kanai-Tajimi power spectral density given by

$$S_{\ddot{x}\ddot{x}}(\omega)=\frac{[1+4\zeta_{g1}^2(\omega/\omega_{g1})^2](\omega/\omega_{g2})^2 s_0^2}{\{[1-(\omega/\omega_{g1})^2]^2+4\zeta_{g1}^2(\omega/\omega_{g1})^2\}\{[1-(\omega/\omega_{g2})^2]^2+4\zeta_{g2}^2(\omega/\omega_{g2})^2\}} \tag{1}$$

in which, ω_{g1}, ζ_{g1}, ω_{g2} and ζ_{g2} are ground motion parameters chosen to be 6 Hz, 0.58, 35 Hz and 0.45, respectively, and S_0 is the intensity to be chosen to match the peak velocity of the measured ground motion. The ground motion spectrum in Eq. (1) has dominant frequencies in the range of 6 to 35 Hz and a stationary ground motion time-history of 15 seconds duration has been simulated using Eq. (1). Then, the simulated stationary ground acceleration is multiplied by an envelope function, $\psi(t)=t^2/25$ for $t \le 5$ sec., $\psi(t)=1$ for $5 < t < 10$ and $\psi(t)=(15-t)^2/25$ for

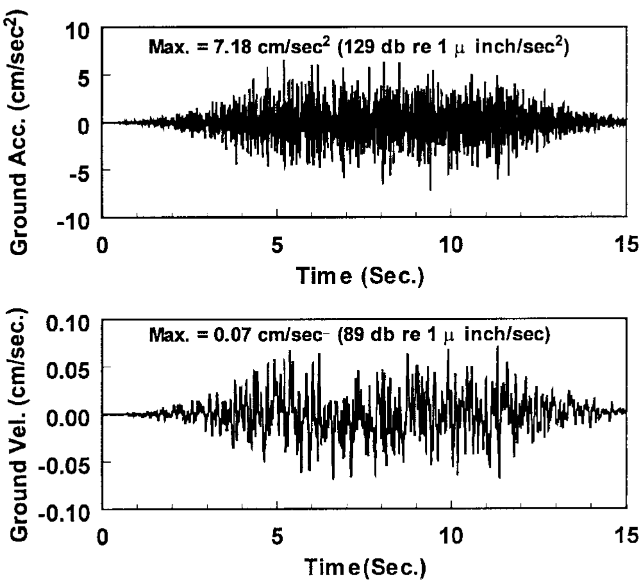

Fig. 2 Time-histories of ground acceleration and velocity for site intensity (A)

$t \geq 10$ sec, to simulate the nonstationary ground acceleration time-history. Further, S_0 in Eq. (1) has been chosen such that the peak ground acceleration is 7.18 gals and the peak velocity is 0.07 cm/sec. Fig. 2 shows the time-history plots for the simulated ground acceleration and velocity, referred to as Sites Intensity (A).

3. Floor response and velocity spectrum

3.1. Equation of motion

Consider an n-dof linear building structure subject to a horizontal ground acceleration $\ddot{x}_0(t)$. The vector equation of motion for the building equipped with r control systems can be expressed as

$$M\ddot{X}(t)+KX(t)+C\dot{X}(t)=HU(t)+\eta\ddot{x}_0(t) \tag{2}$$

where M, K and C are $(n\times n)$ mass, stiffness and damping matrices, respectively, $X(t)=[x_1, x_2, ..., x_n]^T$ is an n displacement vector with x_i being the displacement of the ith floor with respect to the ground, H is a $(n\times r)$ controller location matrix, $U(t)=[u_1(t), u_2(t), ..., u_r(t)]^T$ is a r-vector with $u_i(t)$ being the control force from the ith controller, η is an n-excitation influence vector, and the superscript T denotes the transpose of a vector or a matrix. In the state-space, the equation of motion can be written as

$$\dot{Z}(t)=AZ(t)+BU(t)+E\ddot{x}_0(t) \tag{3}$$

where $Z(t)=[X(t)^T, \dot{X}(t)^T]^T$ is a $2n$-state vector, A, B and E are $(2n\times 2n)$, $(2n\times r)$ and $(2n\times 1)$ matrices, respectively, given by

$$A=\begin{bmatrix} 0 & I \\ -M^{-1}K & -M^{-1}C \end{bmatrix}; \quad B=\begin{bmatrix} 0 \\ M^{-1}H \end{bmatrix}; \quad E=\begin{bmatrix} 0 \\ M^{-1}\eta \end{bmatrix} \tag{4}$$

The state-space equation in Eq. (3) will be used to design appropriate controllers $U(t)$ for the hybrid protection of the building against microvibration.

3.2. Protective systems

To reduce the level of microvibration for floors and buildings, various protective systems in the following will be investigated for their effectiveness, performance and practicality: (i) passive base isolation systems, (ii) hybrid base isolation systems, (iii) passive floor isolation systems, (iv) hybrid floor isolation systems, (v) active protective systems, and (vi) passive energy dissipation systems. Rubber bearing isolators will be used for the passive base isolation system. For hybrid base isolation systems, actuators will be connected in parallel with rubber-bearing isolators as shown in Fig. 3(b). Either rubber-bearings or springs can be used for passive floor isolation system. Again, for the hybrid floor isolation system, actuators will be installed along with the passive floor isolation system, see Fig. 3(c). Active bracings can be used for the active protective system, as shown in Fig. 3(a). Energy dissipation systems, such as viscous dampers and viscoelastic dampers, can also be installed in various story units of the building, Fig. 3(a).

For the protection of equipments and building against both microvibration and earthquake, two additional protective systems that are very effective will be investigated, i.e., passive hybrid base isolation systems and passive hybrid floor isolation systems. The passive hybrid base isolation system consists of stand-by viscous dampers and the same base isolators used for microvibration, whereas the passive hybrid floor isolation system consists of stand-by viscous dampers and the same floor isolators used for microvibration. Stand-by viscous dampers are activated only by earthquake excitations.

For passive protective systems, the control vector $U(t)$ in Eq. (3) is zero. For hybrid or active protective systems, the control vector $U(t)$ should be determined using a control method (e.g., Yang *et al.* 1991, 1992, 1995a, b, 1996a, b, 1997, Spencer and Sain 1997) as will be described later. After the control vector is determined, the floor response time histories, including displacement, velocity

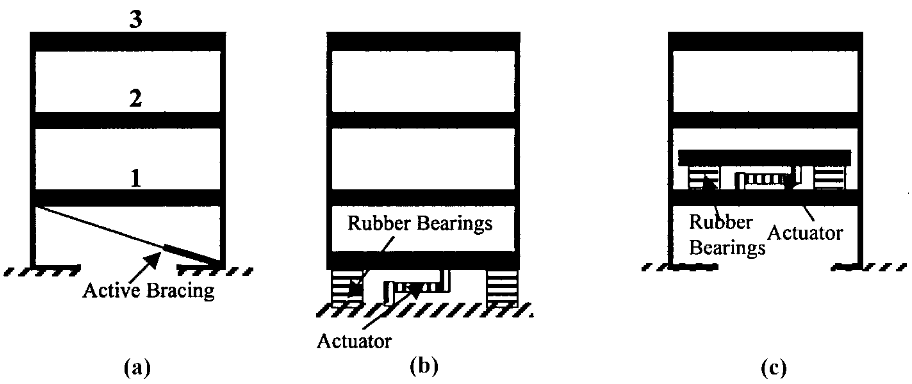

Fig. 3 Building models: (a) Building with active controller; (b) Building with passive and hybrid base isolation systems; and (c) Building with passive and hybrid floor isolation systems

and acceleration, can be computed by numerically integrating Eq. (3).

3.3. Construction of floor velocity spectrum

Generic vibration criteria, known as BBN criteria, have been developed for allowable microvibration levels for sensitive equipments (e.g., Gordon 1991). The main feature of these criteria is the use of velocity spectrum, instead of displacement or acceleration spectrum. BBN criteria are expressed by straight lines on velocity vs. one-third octave frequency plots as shown in Fig. 1, in which the velocity spectrum is expressed in db referenced to 1 μ inch/sec.

For a given velocity response time-history obtained from Eq. (3), the one-third octave plot can be obtained either by actual filtering using one-third octave filters or by taking the Fourier transform (e.g., Amick and Bui 1991). An important characteristics of one-third octave filters is that the bandwidth is approximately 23% of the center frequency, and three adjacent bands represent one octave, i.e., doubling of frequency. The center frequency of a band of one-third octave filter is given by $f_c=2^{(m/3)}$ where m is an integer, for example, f_c=4.0 Hz for m=6. The one-third octave plot of any velocity response time-history $\dot{x}(t)$ can be obtained from its Fourier transform $X(f)$ in approximation as follows

$$X_{1/3}(f_c)=\left[\sum_{0.89f_c}^{1.12f_c}|X(f)|^2\Delta f\right]^{1/2} \tag{5}$$

where Δf is the frequency resolution of *FFT*. The one-third octave plot obtained from Eq. (5) is constant in the frequency band from $0.89f_c$ to $1.12f_c$, and it can be plotted as a histogram.

The magnitude $X_{1/3}(f_c)$ in Eq. (5) is expressed in db referenced to 1 μ inch/sec. The resulting db value, denoted by $Y(f_c)$, is obtained as

$$Y(f_c)=20\log_{10}[X_{1/3}(f_c)/\bar{x}_0] \tag{6}$$

where $\bar{x}_0=1$ μ inch/sec. For instance, the constant velocity of 41.938 db for the 125 μ inch/sec *VC-E* curve in Fig. 1 is obtained as 20 $\log_{10}(125)$=41.938 db. The ground velocity spectrum expressed in db for the ground velocity time history shown in Fig. 2, Site Intensity (A), is plotted as a dashed

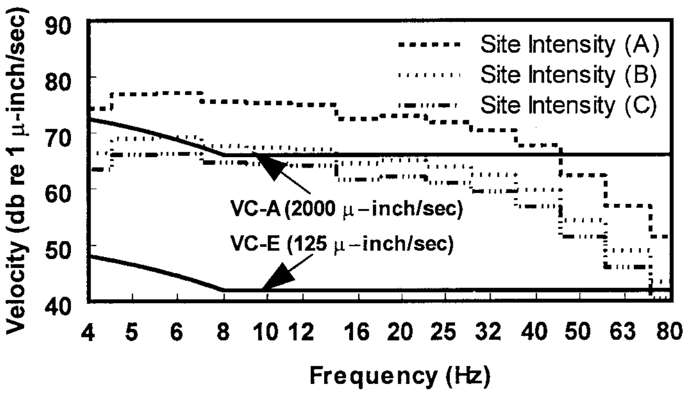

Fig. 4 Velocity spectra of three site intensities

curve in Fig. 4 along with the design criteria for *VC-A* and *VC-E* categories (solid curves). It is observed that the ground velocity spectrum far exceeds the design specification for the floor velocity spectrum for *VC-E* facilities.

4. Performance of protective systems for microvibration

4.1. Building properties

A three-story building model, approximately 22 m × 22 m in plan, is considered for investigating the performance of protective systems for microvibration reduction. The properties of the building are as follows: (i) mass m_i(i=1, 2, 3)= 350.25, 262.69 and 175.13 metric tons, (ii) stiffness k_i(i=1, 2, 3)=4728400, 315230 and 157610 kN/cm, and (iii) viscous damping coefficients c_i(i=1, 2 3)=4369, 291.3, 145.6 kN·sec/cm. The natural frequencies of the building are 3.447, 7.372 and 19.155 Hz, and the corresponding damping ratios are 1%, 2.14% and 5.56%, respectively. The building properties above resemble that of the semiconductor facility where the first story unit is quite stiff, since the first floor is for the clean rooms.

The first floor will be used to operate sensitive equipments in the *VC-E* category shown in Fig. 1. The velocity spectrum of the first floor of the three-story building (fixed-base) under Site Intensity (A) is shown in Fig. 5 by a dotted curve. It is observed that the level of microvibration of the first floor far exceeds the specification for any type of high technology equipments. Hence, additional measures must be taken to reduce the level of floor microvibration.

4.2. Passive and hybrid floor isolation systems

We first consider the passive rubber-bearing isolator, that behaves elastically under microvibration, for the isolation of the first floor as shown in Fig. 3(c). The additional mass on the top of rubber-bearings is one fourth of the first floor mass, i.e., m_d=87.56 tons. Hence, the entire building has four degrees of freedom. The stiffness k_d of rubber-bearings is designed such that the frequency of the

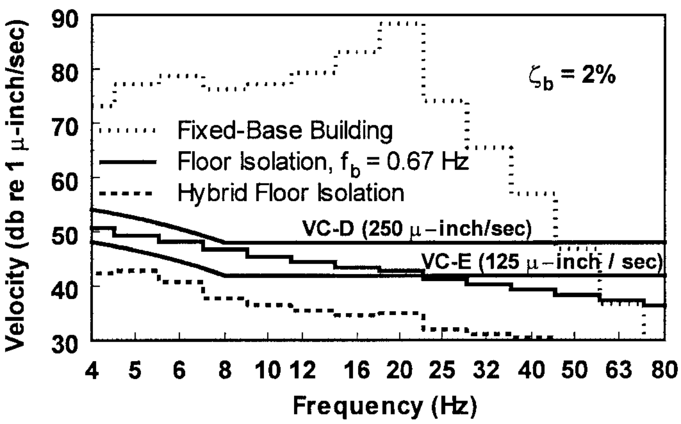

Fig. 5 Velocity spectrum of first floor for building with passive and hybrid floor isolation systems for site intensity (A)

isolator $f_b=(k_d/m_d)^{1/2}=0.67$ Hz, and the damping ratio $\zeta_b=c_d/(4\pi m_d f_d)=2\%$. With such an isolation system for the first floor, the velocity spectrum of the first floor under Site Intensity (A) is presented in Fig. 5 as a solid curve. As observed from Fig. 5, a drastic reduction of the velocity spectrum has been achieved by the installation of such a passive floor isolation system.

Since the performance of the isolation system depends on the isolator frequency f_b and the damping ratio ζ_b, a parametric study has been conducted. Extensive simulation results indicate that the lower the isolator frequency f_b, the better the performance. In other words, the velocity spectrum can be reduced more effectively by lowering the isolator frequency. However, as the isolator frequency f_b reduces, the drift of the isolation system increases, and f_b is also subject to practical limitations. Simulation results further demonstrate that the performance of the isolation system degrades with the increase of the damping ratio ζ_b, i.e., the smaller ζ_b is used, the better (smaller) the velocity spectrum is obtained. In the other words, damping increases the absolute velocity response. Again, the lowest value of ζ_b is also subject to practical limitation of rubber-bearings.

Note that the passive floor isolation system satisfies the design specification for VC-D facilities but not for VC-E facilities. Consequently, the isolator frequency f_b should be reduced. If the reduction of f_b is not practical, another approach is the use of hybrid floor isolation system by adding actuators in parallel to rubber bearings, see Fig. 3(c). In this case, a linear controller is designed for the active control force $U=-Gy$ where $y=[y_1,\ \dot{y}_1]^T$ is the measured output with y_1 and $\dot{y}_1$ being the drift and velocity of the floor isolator. A static output feedback gain matrix $G=[-373.36,\ -1.9]$ is designed using the static output pole placement method (Davison 1970). The resulting floor velocity spectrum using the hybrid floor isolation system with $f_b=0.67$ Hz and $\zeta_b=2\%$ is presented in Fig. 5 as a heavy dotted curve, where the peak control force is 4 kN. As observed from Fig. 5, the velocity spectrum satisfies the design specification for VC-E facilities. Such a hybrid floor isolation system can be achieved by using one electric or magnetostrictive actuator (e.g., Nakamura *et al.* 1999). Hence, the hybrid floor isolation system is very effective and practical for the protection of high-tech facilities against microvibrations.

Suppose the site of the building is moved farther from the railway track such that the magnitudes of time histories of the ground motions shown in Fig. 2 are reduced by 2.5 times. The resulting peak ground acceleration is 2.87 gals and the peak velocity is 0.028 cm/sec, referred to as Site Intensity (B). The velocity spectrum of Site Intensity (B) is shown in Fig. 4 as a dotted curve. The resulting velocity spectrum of the first floor of the fixed-base building is plotted in Fig. 6 as a dotted curve. As observed from Fig. 6, the velocity spectrum for the fixed-base building does not satisfy the design specification for any high-tech facility. Consequently, the passive floor isolation system described above, i.e., $f_b=0.67$ Hz and $\zeta_b=2\%$, is implemented. In this case, the resulting velocity spectrum of the first floor is presented in Fig. 6 as a solid curve. It is observed that the passive floor isolation system satisfies the design specification for VC-E facilities.

4.3. Passive and hybrid base isolation systems

Instead of isolating the floor, another possible approach is to isolate the building at the base. Consider rubber-bearing base isolators with an additional base mass of $m_d=500$ tons as shown in Fig. 3(b). The frequency of base isolators f_b is defined by $f_b=(k_d/\overline{m})^{1/2}$, where $\overline{m}=m_d+m_1+m_2+m_3$ is the total mass of the building including the additional base mass. The stiffness k_d of the base isolation system is designed such that the frequency of base isolators is $f_b=0.67$ Hz, and the corresponding damping ratio $\zeta_b=c_d/(4\pi\overline{m} f_d)=2\%$. For the building equipped with such a base

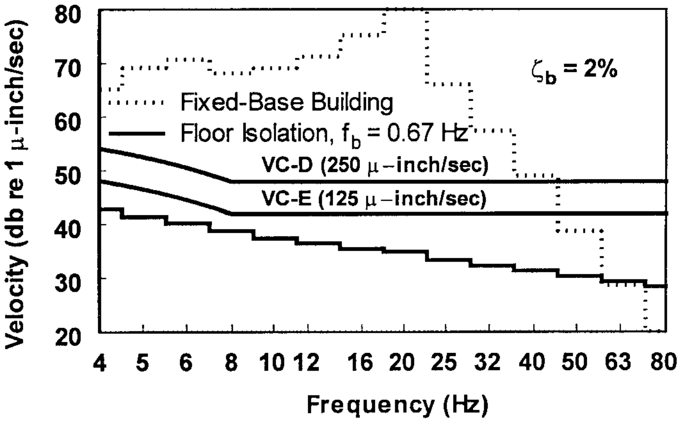

Fig. 6 Velocity spectrum of first floor for building with passive floor isolation system for site intensity (B)

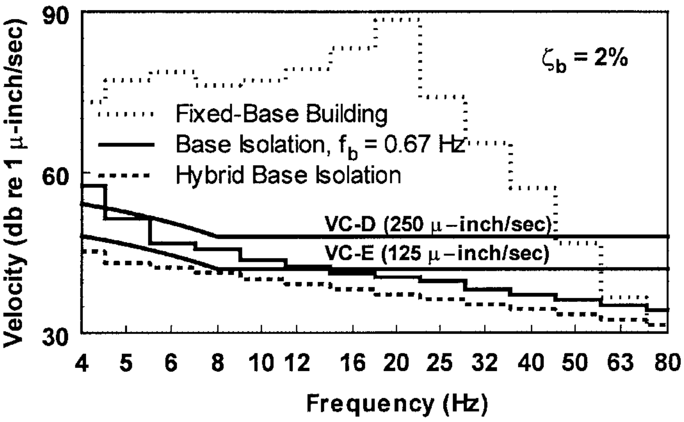

Fig. 7 Velocity spectrum of first floor for building with passive and hybrid base isolation systems for site intensity (A)

isolation system and subject to microvibration with Site Intensity (A), the velocity spectrum of the first floor is presented in Fig. 7 by a solid curve. Also shown in Fig. 7 as a dotted curve is the corresponding velocity spectrum of the fixed-base building without base isolators for comparison. As observed from Fig. 7, a drastic reduction for the velocity spectrum has been achieved by the use of passive rubber-bearing base isolators. However, such a base isolation system does not satisfy the design specifications for VC-D and VC-E facilities.

The sensitivity for the performance of the passive base isolation system with respect to the isolator frequency f_b and the damping ratio ζ_b has been studied. Extensive simulation results indicate that the velocity spectrum of the floor response reduces drastically with respect to the decrease of the isolator frequency f_b. On the other hand, the magnitude of the velocity spectrum increases with the increase of damping ratio ζ_b. The results of this sensitivity study is the same as that for the passive floor isolation system. Hence, it is concluded that the only way to reduce the velocity spectrum is to decrease the isolator frequency, since the increase of damping in the isolation system degrades the performance of the passive base isolation system against microvibration.

Consequently, to further reduce the velocity spectrum in order to satisfy the design specification for VC-E facilities, the isolator frequency f_b should be reduced. However, the frequency $f_b=(k_d/\overline{m})^{1/2}$ of 0.67 Hz for the base isolation system is quite low already. Hence, we shall consider the use of hybrid base isolation system (e.g., Yang *et al.* 1992, 1995) by attaching actuators to rubber-bearing isolators. A linear controller $U=-Gy$ has been designed using the static output pole placement method (Davison 1970), where $y=[y_b,\ \dot{y}_b]^T$ is the measured output with y_b being the drift of base isolators. The gain matrix G=(−20643, −153) is designed such that the velocity spectrum of the first floor satisfies the design specification for VC-E facilities as shown in Fig. 7 by a dashed curve. In this case, the peak control force required of the actuators is 379 kN. With the installation of four actuators, the required capacity for each actuator is about 95 kN. The installation of such big hydraulic actuators for the reduction of microvibration may not be desirable.

If the building facility is moved further away from the railway track with Site Intensity (B), the velocity spectra of the first floor for: (i) the fixed-base building, and (ii) the base isolated building with f_b=0.67 Hz and ζ_b=2% are presented in Fig. 8 by a dotted curve and a solid curve, respectively. As observed from Fig. 8, the passive base isolation system satisfies the design specification in the frequency range larger than 4.5 Hz. Again, the hybrid base isolation system is considered and designed such that the velocity spectrum satisfies the design specification as shown in Fig. 8 by a dashed curve. In this case, a linear gain matrix G=(−4413, −23) has been obtained and the required peak control force is 17.3 kN. Consequently, the installation of four electric actuators, each with a capacity of 4.5 kN is reasonable.

Suppose the building facility is further moved away from the railway track such that the velocity spectrum of the ground motion is slightly below the VC-A category as shown in Fig. 4 by a dash-dotted curve, referred to as the Site Intensity (C). Then, the floor velocity spectra of the fixed-base building and the building equipped with the passive base isolation system with f_b=0.67 Hz and ζ_b=2% are shown in Fig. 9 by a dotted curve and a dashed curve, respectively. As observed from Fig. 9, the installation of the passive base isolation system satisfies the design specification for VC-E facilities.

4.4. Passive energy dissipation systems and active protective systems

While damping has a significant influence on the dynamic response quantities of seismic-excited

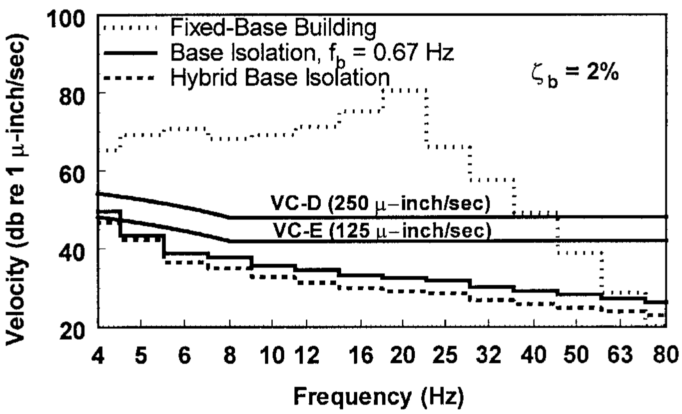

Fig. 8 Velocity spectrum of first floor for building with passive and hybrid base isolation systems for site intensity (B)

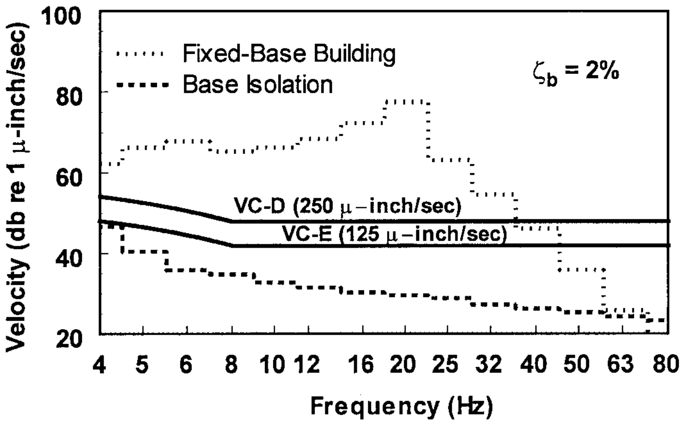

Fig. 9 velocity spectrum of first floor for building with passive base isolation system for site intensity (C)

buildings, its influence on the microvibration of buildings, in particular on the absolute velocity and acceleration of floors, is minimal. This is evidenced by extensive simulation results using different values of damping ratios ζ_1 and ζ_b for the first mode of the building and the isolation system, respectively. Due to space limitation, the numerical results are not presented. One reason is that for the damping force to be effective, the interstory velocity should be large, which is not the case in microvibration. Another reason is that damping dissipates energies to reduce the deformations (interstory drift, velocity and acceleration) rather than the absolute displacements, velocity and acceleration. If the velocity spectrum of the ground excitation exceeds the design specification for the floor velocity spectrum, which is the case considered above, an increase of either stiffness or damping is useless. Consequently, passive energy dissipation systems, such as viscous dampers, viscoelastic dampers and others, are not effective for reducing the microvibration of high technology facilities. In a similar reasoning, the semi-active dampers, which utilize the deformation of the structure to either dissipate energies or to produce resisting forces, may not be effective.

Finally, active control systems, such as active bracing systems, etc., are not suitable for the reduction of microvibration when the velocity spectrum of ground excitation exceeds the design specification of a particular facility of interest. Simulation results demonstrate that the required active control force is too big to be practical. Due to space limitations, simulation results in this subsection are not presented.

5. Protective systems for both microvibration and earthquake

If high-tech facilities are located in the active seismic region, the response of these facilities due to earthquakes should be considered. In particular, the effect of the installation of protective systems against microvibration should be investigated. As presented previously, both passive base isolation and floor isolation systems with f_b=0.67 Hz and ζ_b=2% can be used to significantly reduce the level of microvibration. To investigate the effect of installing these passive isolation systems on seismic responses, the building is subject to a 0.3 g El Centro earthquake. The response quantities, including the peak drifts y_i of the ith story unit and the peak absolute acceleration $\ddot{x}_{ai}$ of the ith floor, for the fixed-base building (without isolation system) are presented in Columns (2) and (3) of Table 1.

Table 1 Peak response quantities of building equipped with different protective systems and subject to 0.3 g El Centro Earthquake

Floor (1)	Fixed base		Base isolation: Base-isolation, ζ_b=2%		Base isolation: Passive hybrid base-isolation (c_b=1431 kN·sec/cm)		Floor (8)	Floor isolation: Floor-isolation, ζ_b=2%		Floor isolation: Passive hybrid floor-isolation (c_b=96 kN·sec/cm)	
	y_i (cm) (2)	$\ddot{x}_{ai}$ (cm/s^2) (3)	y_i (cm) (4)	$\ddot{x}_{ai}$ (cm/s^2) (5)	y_i (cm) (6)	$\ddot{x}_{ai}$ (cm/s^2) (7)		y_i (cm) (9)	$\ddot{x}_{ai}$ (cm/s^2) (10)	y_i (cm) (11)	$\ddot{x}_{ai}$ (cm/s^2) (12)
BI	–	–	10.83	186	6.72	121	FI	10.65	187	6.76	125
1	0.07	308	0.03	187	0.02	122	1	0.07	308	0.07	308
2	0.87	681	0.28	195	0.18	128	2	0.87	680	0.87	680
3	1.24	1110	0.23	203	0.15	136	3	1.24	1110	1.24	1110

Under seismic excitations, the safety of the building and high-tech equipments is of primary concern, whereas the serviceability (velocity spectrum) is most important in microvibration. Hence, the peak interstory drifts and peak accelerations are shown in Table 1. As observed from Table 1, the peak drifts may be acceptable. However, the peak floor accelerations are quite high and the peak acceleration of the first floor, on which precision equipments are installed, is about 0.3 g.

When the building is installed with a passive base isolation system with f_b=0.67 Hz and ζ_b=2%, the peak response quantities are presented in Column (4) and (5) of Table 1. In Table 1, the first row denoted by "BI" represents the peak response quantities of the base isolation system, for instance y_B represents the peak drift of rubber-bearing isolators. The results demonstrate that the peak response quantities of the entire building have been significantly reduced. The only concern is the peak drift of rubber-bearing base isolators which is 10.83 cm. If such a drift is not acceptable, it can be reduced by installing passive viscous dampers in the base isolation system to increase the damping ratio, referred to as passive hybrid base isolation system. With the passive hybrid base isolation system, peak response quantities of the building are presented in Columns (6) and (7) of Table 1, in which the total capacity of viscous dampers is 1431 kN.sec/cm. As observed from Table 1, all the peak response quantities of the building have been further reduced by the installation of viscous dampers, where the peak drift of base isolators is 6.72 cm and the peak acceleration of the first floor is 122 cm /sec^2.

Peak response quantities of the building equipped with a passive floor isolation system with f_b=0.67 Hz and ζ_b=2% are shown in Columns (9) and (10) of Table 1. The results indicate that the response quantities of the building structure itself remain the same as that of the fixed-base building. However, the peak acceleration of the isolated floor for precision equipments has been reduced from 308 cm/sec^2 to 187 cm/sec^2, whereas the peak drift of floor isolators is 10.65 cm. If the peak drift of the floor isolation system is not acceptable, then passive viscous dampers can be attached to it, referred to as the passive hybrid floor isolation system. Peak response quantities of the building equipped with such a passive hybrid floor isolation system are shown in Columns (11) and (12) of Table 1, in which the required total capacity of passive viscous dampers is 96 kN·sec/cm. As observed from these results, not only is the peak drift of the floor isolation system reduced, but also the peak acceleration of the isolated floor is reduced from 187 cm/sec^2 to 125 cm/sec^2. Likewise, other building response quantities remain unchanged. It should be noted that unlike the mitigation of microvibration, added damping has a significant benefit in protecting structures against earthquakes.

The results presented above demonstrate that the same passive floor isolation system and passive base isolation system, which are very effective for the mitigation of microvibration, are also effective for protecting high-tech equipments against earthquakes. Significant benefit can be achieved further by installing passive viscous dampers to these isolation systems. These passive viscous dampers should be installed in the isolation systems as stand-by units. These stand-by dampers are activated only by earthquakes, and they are inactive during microvibration. Likewise, these stand-by passive viscous dampers can also be installed in parallel with actuators in the hybrid floor isolation system and hybrid base isolation system presented in Subsections 4.2 and 4.3.

6. Conclusion

Preliminary studies have been conducted of the possible applications of different protective systems to high-technology facilities for the reduction of microvibration. In particular, passive and hybrid base isolation systems, passive and hybrid floor isolation systems, active protective systems, and passive energy dissipation systems have been investigated. Under seismic excitations, the effectiveness of protective systems, that are designed for microvibration, to mitigate earthquake responses have also been investigated.

For the mitigation of microvibration alone, it is found that passive energy dissipation systems, such as viscous dampers, viscoelastic dampers, etc., are not useful. An increase of damping in the building does not reduce the response velocity (absolute) spectrum under microvibration, when the intensity of the site excitation (velocity spectrum) exceeds the design specification for the floor. As a result, lowering the frequency of the building or the critical floor becomes the only feasible solution to reduce microvibration. This renders the active control systems impractical, because the required control force is too high. Both passive floor isolation systems and passive base isolation systems are shown to be very effective in reducing microvibration, due to the frequency reduction of either the building or the floor. If the site intensity is high, hybrid floor isolation systems, consisting of passive floor isolators and small electric actuators, are effective and practical. In general, hybrid or passive floor isolation systems are superior to passive or hybrid base isolation systems in satisfying the design specification for microvibration.

If high-tech facilities are located in the active seismic zone, in addition to the reduction of microvibration, protection against earthquakes is also an important consideration. The following conclusions are obtained from the current study. The same passive floor isolation system and passive base isolation system, which are very effective for the mitigation of microvibration, are also effective for protecting high-tech precision equipments against seismic events. Passive hybrid base isolation systems, consisting of passive base isolators and stand-by passive viscous dampers (to be activated only during seismic events), are very effective in protecting both high-tech equipments (floor) and the entire building. Passive hybrid floor isolation systems, consisting of passive floor isolators and stand-by passive viscous dampers (to be activated only during seismic events), are very effective in protecting only high-tech equipments (floor) but not the building. Consequently, if the seismic design of the building is adequate, passive hybrid floor isolation systems are superior; otherwise passive hybrid base isolation systems should be used.

Acknowledgment

This research is supported by National Science Foundation through Grant No. CMS-96-25616 and PSC-CUNY Research Award No. 669646. Valuable discussion with Dr. Y.C. Ho of Science Park Administration, Taiwan, is gratefully acknowledged.

References

Amick, H. and Bui, S.K. (1991), “A review of several methods for processing vibration data”, *SPIE*, **1619**, 253-264.

Andow, K. and Ogawa, Y. (1998), “Predicting microvibration at a semiconductor plant near a high-speed railway”, *Workshop on Effect of High-Speed Vibration on Structures and Equipment*, Taiwan, 57-62.

Davison, E. J. (1970), “On pole assignment in linear systems with incomplete state feedback”, *IEEE Transactions on Automatic Control*, **AC-15**(3), 348-51.

Dawn, T.M. and Stanworth, C.G. (1979), “Ground vibrations from passing trains”, *Journal of Sound and Vibration*, **66**(3), 355-362.

Gordon, C.G. (1991), “Generic criteria for vibration sensitive equipment”, *SPIE*, **1619**, 71-85.

Heckl, M., Hauck, G. and Wettschureck, R. (1996), “Structure-borne sound and vibration from rail traffic”, *Journal of Sound and Vibration*, **193**(1), 175-184.

Heiland D. and Beyer K. (1998), “Vibrations in semiconductor fabs”, Workshop on Effect of High-Speed Vibration on Structures and Equipment, 63-76, Taiwan.

Ho, Y.C (1997), “Vibration prevention of high speed train near semiconductor facility in Tainan science-based industry park”, *Symposium for Environmental Technologies and Strategies in Semiconductor Industry*, 67-73, Tokyo, Japan.

Hunt, H.E.M. (1996), “Modelling of rail vehicles and track for calculation of ground-vibration transmission into buildings”, *Journal of Sound and Vibration*, **193**(1), 185-194.

Iseki, Y. (1997), “Counter measure of semiconductor factory for earthquake”, *Symp. for Environ. Technologies and Strategies in Semiconductor Industry*, 82-88, Tokyo, Japan.

Jones, C.J.C. and Block, R. (1996), “Prediction of ground vibration from freight trains”, *Journal of Sound and Vibration*, **193**(1), 205-213.

Krylov, V.V. (1996), “Vibration impact of high-speed trains I, effect of track dynamics”, *J. Acoustical Society of America*, **100**(5), 3121-3134.

Kuppelwieser, H. and Ziegler, A. (1996), “A tool for predicting vibration and structure-borne noise emissions caused by railways”, *J. of Sound and Vibration*, **193**(1), 261-267.

Liu, S.C. (1998), “NSF’s infrastructure systems research program and high-speed ground transportation research”, *Workshop on Effect of High-Speed Vibration on Structures and Equipment*, Taiwan, 1-15.

Madshus, C., Bessason, B. and Harvik, L. (1996), “Prediction model for low frequency vibration from high speed railways on soft ground”, *J. Sound and Vibration*, **193**(1), 195-203.

Nakamura, Y. *et al.* (1999), “Development of 6-DOF microvibration control system using giant magnetostrictive actuator”, *SPIE*, **3671**, Paper No. 24.

Nelson, J.T. (1996), “Recent developments in ground-borne noise and vibration control”, *Journal of Sound and Vibration*, **193**(1), 367-376.

Spencer, B.F., Jr. and Sain, M.K. (1997), “Controlling buildings: A new frontier in feedback”, *IEEE Control Systems*, **17**(6), 19-35.

Takemiya, H. (1998), “Lineside ground vibrations induced by high speed train passage”, *Workshop on Effect of High-Speed Vibration on Structures and Equipment*, Taiwan, 43-49.

Takemiya, H. and Kellezi, L. (1998), “Paraseismic behaviour of wave impeding block measured for ground vibration reduction”, *Workshop on Effect of High-Speed Vibration on Structures and Equipment*, Taiwan, 51-56.

Ungar, E.E., Starz. D.H. and Amick, C.H. (1990), "Vibration control design of high technology facilities", *Sound and Vibration*, **24**(7), 20-27.

Verhas, H.P. (1979), "Prediction of the propagation of train-induced ground vibration", *Journal of Sound and Vibration*, **66**(3), 371-376.

Yang, J.N., Danielians, A. and Liu, S.C. (1991), "Aseismic hybrid control systems for building structures", *Journal of Engineering Mechanics, ASCE*, **117**(4), 836-853.

Yang, J.N., Li, Z., Danielians, A. and Liu, S.C. (1992), "Hybrid control of nonlinear and hysteretic systems I", *Journal of Engineering Mechanics, ASCE*, **118**(7), 1423-1440.

Yang, J.N., Wu, J.C. and Agrawal, A.K. (1995a), "Sliding mode control of nonlinear and hysteretic structures", *Journal of Engineering Mechanics, ASCE*, **121**(12), 1386-1390.

Yang, J.N., Wu, J.C., Kawashima, K. and Unjoh, S. (1995b), "Hybrid control of seismic-excited bridge structures", *J. Earthquake Engineering and Structural Dynamics*, **24**(11), 1437-1451.

Yang, J.N., Wu, J.C., Reinhorn, A.M., Riley, M., Schmitendorf, W.E. and Jabbari, F. (1996a), "Experimental verifications of H infinity and sliding mode control for seismic-excited buildings", *Journal of Structural Engineering, ASCE*, **122**(1), 69-75.

Yang, J.N., Wu, J.C. and Li, Z. (1996b), "Control of seismic-excited buildings using active variable stiffness systems", *Journal of Engineering Structure*, **18**(8), 589-596.

Yang, J.N., Wu, J.C., Agrawal, A.K. and Hsu, S.Y. (1997), "Sliding mode control with compensators for wind and seismic response control", *J. Earthquake Engineering and Structural Dynamics*, **26**, 1137-1156.

Yang, J.N. and Agrawal, A.K. (1998), "Protective systems for microvibration reduction of buildings," *Proc. of ASIA-Pacific Workshop on Seismic Design and Retrofit of Structures*, August 10-13, Taipei, Taiwan, 319-333.

Yang, J.N. and Agrawal, A.K. (1999), "Protective systems for high-technology facilities against microvibration", *Proc. of US-Korea Workshop on New Frontier in Infrastructural/Seismic Engineering*, August 24-25, Seoul, Korea, Techno-Press, 29-52.

Yang, Y.B. (1998), "Simulation of wave barriers for reduction of train or factory-induced vibration", *Workshop on Effect of High-Speed Vibration on Structures and Equipment*, Taiwan, 77-116.